Intelligent Model for Endpoint Accelerations of Two link Flexible Manipulator Using a Deep Learning Neural Network

Zidan Abdulghani
School of Mechanical Engineering, Universiti Teknologi Malaysia
Skudai, Johor, Malaysia
zidan12990@gmail.com

Intan Z. Mat Darus
School of Mechanical Engineering, Universiti Teknologi Malaysia
Skudai, Johor, Malaysia
intan@utm.my

Annisa Jamali
Faculty of engineering
Universiti Malaysia Sarawak
94300 Kota Samarahan
jannisa@unimas.my

2022 IEEE 8th International Conference on Smart Instrumentation, Measurement and Applications (ICSIMA) | 978-1-6654-8800-6/22/$31.00 ©2022 IEEE | DOI: 10.1109/ICSIMA55652.2022.9928949

Abstract*—This article investigates a two-link flexible manipulator (TLFM) that can be modelled utilizing a deep learning neural network. The system was classified under a multiple-input multiple-output (MIMO) system. In the modelling stage of this study, the TLFM dynamic models were divided into single-input single-output (SISO) models. Since coupling impact was assumed to be minimised, the characterizations of TLFM were defined independently in each model. Two discrete SISO models of a flexible two link manipulator were developed using the torque input and the endpoint accelerations of each link. The input-output data pairs were collected from experimental work and utilised to establish the system model. The Long Short-Term Memory (LSTM) algorithm optimised using Particle Swarm Optimization (PSO) was selected as the model structure due to the system's high degree of nonlinearity. The identification of the TLFM system utilizing LSTM optimised by PSO was successful, according to the high-performance result of PSO. Using LSTM-PSO, it is demonstrated that both link 1 and 2 models are accurately identified and that their performance in terms of MSE for links endpoint acceleration 1 and 2 is within a 95% confidence interval.

Keywords*—Tow link flexible manipulator, Deep learning, Flexible manipulator, LSTM-PSO, Non-parametric modeling

I. INTRODUCTION

Flexible manipulators introduce unwanted vibrations, which are not simple to control because of its high non-linearity. Current research concentrates on enhancing the control schemes to suppress these vibrations. A reliable controller must be developed to keep the advantages linked with the flexibility and lightness of the manipulators, the modeling system's accuracy, and efficiency[1]. Suppressing the vibration on flexible structures is very important. The structure vibration will affect the performance, such as reduced efficiency and accuracy, tracking errors, and lags between tasks. Furthermore, extreme and continuous vibrations will cause the system's early failure and possible deformation [2].

Since the initial emerging of the Long Short-Term Memory (LSTM) network structure in 1997, many theoretical and experimental publications concerning this type of Recurrent Neural Networks (RNN) have been published, describing the great results obtained along a wide range of application fields which mostly sequences data. The fields of language modelling, machine translation, speech to text transcription, and many applications have seen significant advances due to the LSTM network. Researchers have been evaluating the LSTM network's suitability for their research or practical use-cases. The remarkable benchmarks mentioned in the literature served as the motivation behind the decision. The majority of RNN and LSTM network configurations are productively implemented and ready for production in all significant open source machine learning frameworks [3].

LSTM is a RNN architecture created to solve the exploding and vanishing gradient issues in traditional RNN. RNN are effective for simulating sequences because they have cyclic connections, unlike feedforward neural networks [4]. In addition, LSTM is used to create the inverse dynamic of the manipulator F[5]. According to the simulation results, it is essential to prioritise the impacts of the highest number of epochs on model performing for the proposed deep learning architecture. Expectation accuracy will decrease as the number of hidden layers rises, whereas the impacts of hidden nodes on model performing are constrained.

Rueckert and Nakatenus created model of inverse dynamic based on a LSTM with time difficulty. The approach was tested on a KUKA robot arm utilised for object manipulation tasks with varying loads. It was demonstrated that these variation of estimates might be employed to enhance a modify the stiffness or movement representation of the controller[6].

A prediction of LSTM and seq-2-seq structure was applied by Xiang and Yan to estimate hourly rainfall-runoff. The models were calculated using the normalised mean square error, statistical bias, correlation coefficient, and Nash-Sutcliffe Efficiency coefficient [7]. The prediction accuracy could be increased by using the LSTM-seq2seq model, which has a respectable predictive performance. Shen and Njock have suggested a system that incorporates data sequencing and Bi-LSTM in order to expect the jet grouted columns diameter. The findings demonstrate the precision with which the proposed methodologies can calculate the variant in the diameter of column with depth [8].

Gonzalez and Yu made use of the benefits of LSTM and NN in combination. One multilayer perceptron, one hierarchical recurrent network, and a newly used backpropagation through time and backpropagation methods are all components of the innovative neural model[9]. The results showed that the modified LSTM model offered for the simulation model performed noticeably more improved to the other existing neural models. In order to process information in sequences, LSTM additionally makes use of recurrent processes and gate approaches. In comparison to other

feedforward and recurrent NNs, LSTM has a lot of advantages for modelling time series, such as audio and video [10].

LSTM was used in Deep Learning to represent nonlinear dynamic systems, and it produced promising performance in prediction. However, as indicated in studies, LSTM effects are mostly determined by the number of maximum epochs as well as by the number of hidden nodes.

Finding an accurate model of the system that has to be controlled is important for the design of an effective controller. The majority of research focuses on mathematical models like LPM, AMM, FEM, and LM to develop models of flexible manipulators; nevertheless, these models are constrained by the assumptions made for them. Additionally, a lot of research has used system parametric identification techniques, and flexible manipulator modelling is already well developed. Nonparametric identification techniques have, however, received relatively few nonlinear model research. The both numbers of hidden nodes and maximum epochs for LSTM are optimised in this work employing deep learning using LSTM and particle swam optimization (PSO).

II. EXPERIMENTAL SET UP OF TLFM

TLFM test rig was conceived and built by Jamali based on the diagram shown in Fig. 1 to assess the effectiveness of the suggested control methods. The TLFM system consists of two flexible links, data acquisition system, dc motors, motor controllers, accelerometers and power source. Motor controllers are connected to DC motors. Motor controllers are currently coupled to power supplies and connecter blocks [11].

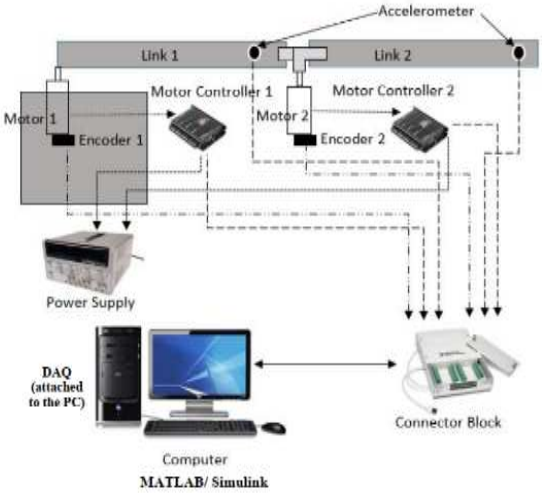

Fig. 1. Two link flexible robotic manipulator rig.

III. EXPERIMENTATION SET UP AND DATA COLLECTION

TLFM performs at each link as a single input multiple output system. The manipulator hub is subjected to a single torque system, which changes the hub angle. The TLFM setup was used to experimentally collect the input-output data. The block diagrams utilised to gather the data are shown in figs. 2 (a) and (b). The power required to simultaneously excite the two-link was provided by using bang-bang signals. Two accelerometers were used for the accumulating. Two outputs, one for each endpoint acceleration of a different link.

The experiment lasted 9 seconds, with a 0.01 second sampling interval. The time needed to move the links to the desired angle is sufficient given the constraints on space and link motion shown in fig. 3. Utilizing MATLAB, the online real-time application is created. The interface between the computer system and signals from input and output is the data acquisition system (NI-DAQ). Through NI-DAQ, the motor driver receives the actuation signal from the encoder as well as the motor driver's digital input.

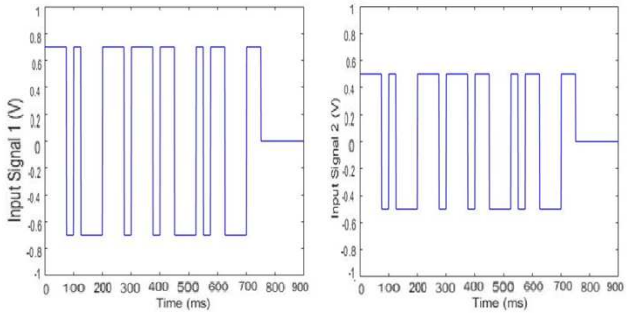

(a) Flexible manipulator link 1 (b) Flexible manipulator link 2

Fig. 2. Bang-bang input voltage.

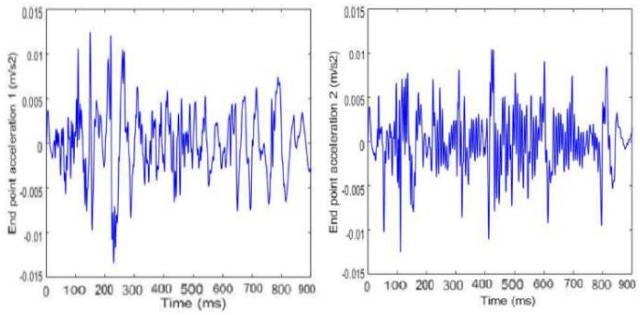

(a) Endpoint acceleration 1 (b) Endpoint acceleration 2

Fig. 3. Experimental output response.

IV. MODEL STRUCTURE OF DEEP LEARNING LSTM

The two-link flexible manipulator is predicted using a deep learning system. There are various units in the deep learning model. The computational unit, which is made up of several layers, is designed to successively obtain greater features from the input data. By eliminating duplicate data from each input and choosing only the characteristics that enhance performance, so every layer performs a different task to extract link for more information from the data analysis[12].

The proposed LSTM model consists of four layers: the sequence input layer, LSTM layer, fully connected layer, and regression layer respectively in fig. 4, these connections between the layers are made gradually. The data sequence found in the first row of a data matrix provides input to the sequence input layer. It is analysed by the LSTM layer. The LSTM layer is discussed in more detail in long short-term memory. The input data that are simulated by the LSTM layer are then presented to the fully connected layer. Similar to a

standard feedforward network, this layer conveys the sequence of crucial information to the layer below.

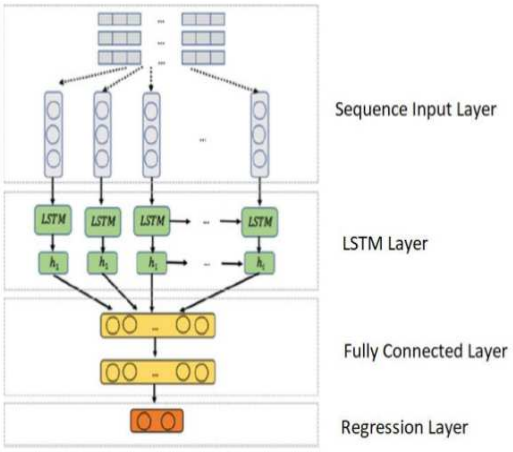

Fig. 4. Model Structure of Deep Learning LSTM [13]

A. Deep Learning LSTM Optimized by PSO

Particle swarm optimization features a built-in guidance strategy that enables PSO solutions to learn from better solutions and utilise that information to generate their own unique solutions. In this case study, the PSO was chosen to optimise the LSTM maximum epoch and neuron nodes because it provides a faster convergence rate with a higher probability.

The proper model for TLFM is found in this paper by combining the methodologies of deep learning LSTM and particle swarm optimization. The maximum epoch and neuron nodes make up the PSO position, according to flow chart fig. 5. For the TLFM system's prediction outputs, this position takes into account the LSTM training's parameters. It is the fitness function of PSO to calculate mean square error (MSE) from the original outputs and the predicted outputs. Since each particle is being evaluated objectively, LSTM is used.

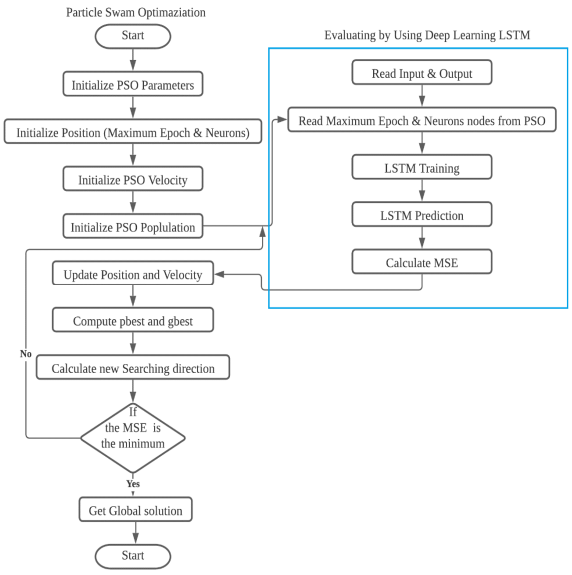

Fig. 5. Flow chart of deep learning LSTM optimized by particle swarm optimization algorithm.

V. RESULTS AND DISCUSSION

Various MATLAB sequencers, including deep learning LSTM and neural networks models for simulating endpoint acceleration, were created utilising system identification. The models employed the data collected through the input voltage to the endpoint acceleration output from the TLFM equipment as detailed in this paper. The data set's 900 data were divided into 2 sets, each with 650 and 250 records. The model was created using the first set (the prediction set), and the validation test was carried out using the second set (the testing set) for validation purposes [14, 15]. On the deep learning LSTM, the particle swam optimization (PSO) approach has been used to find the right number of maximum epochs and neurons.

A. Endpoint acceleration

The system identification procedure utilising deep learning LSTM was explored by varying the number of maximum epochs and neuronal nodes to determine the boundary of searching that can be utilised to start the particle swam. The outline of effectiveness for endpoint accelerations 1 and 2 is shown in Table 4.2. It can be seen through the table that for output and input data sets for both endpoint accelerations 2 and 1, the MSE decreased between 250 and 500 for the maximum epoch and between 150 and 300 for the maximum number of neuronal nodes. Then, the value of MSE in endpoint accelerations 1 decreased into 0.0754 between 300 to 450 neurons nodes. Therefore, it has been shown that the maximum epoch range of 500 to 800 and the number of neuronal nodes of 200 to 500 are used to obtain the good prediction.

TABLE I. PERFORMANCE OF DEEP LEARNING LSTM FOR ENDPOINT ACCELERATIONS WITH DIFFERENT NUMBER OF MAXIMUM EPOCH AND THE NUMBER NEURONS NODES

Endpoint Accelerations 1			**Endpoint Accelerations 2**		
Maximum of epoch	***Neuron's nodes***	***MSE***	***Maximum of epoch***	***Neuron's nodes***	***MSE***
250	150	0.087	250	150	0.012
500	300	0.0787	500	300	0.0071
750	450	0.0954	750	450	0.092
1000	600	0.1242	1000	600	0.085

Then, deep learning LSTM is tested with various number of maximum epoch and the number neurons nodes. Thus, the boundary that will search for the number of maximum epochs 500 to 800 and the number neurons nodes 200 to 500. PSO has been used to search for the MSE fitness function of the algorithm as shown at the fig. 6.

In PSO for both endpoint accelerations 1 and 2, the initialization of the particle sawm was 22 of the population and 50 iterations. The constant values of PSO were 0.75 for W and 2 for C1 and C2. Thus, the mean square error (MSE) for endpoint accelerations 1 is 0.00016 at the maximum number of epoch 399 and neurons node 703. Moreover, MSE of the endpoint accelerations 2 is 0.000425 at the maximum number of epoch 261 and neurons node 526.

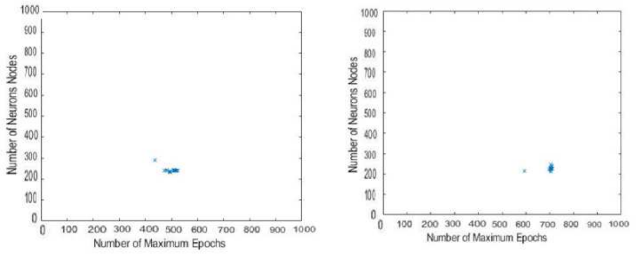

(a) Endpoint accelerations 1 (b) Endpoint accelerations 2

Fig. 6. Searching Swam of MSE fitness function.

The LSTM-PSO predictions of the endpoint accelerations are shown in figs. 7 (a) and 8 (a). A green vertical line at the position 650 represents the validated data. Both plots show that although LSTM-PSO can track actual data, there is a large variance between predicted data and actual data. The divergence is significantly more obvious in the section with validated data. Both plots show that although LSTM-PSO can track actual data, there is a difference between predicted data and actual data. The divergence is significantly obvious in the section with validated data. These are supported by figs. 7 (b) and 8 (b), which show the inaccuracy between the real and predicted LSTM-PSO. The error is significant and cannot be ignored. As shown in figs. 9 and 10, the correlations of the error for the two LSTM-PSO models obviously deviate from the 95% confidence level. It has been proven that the LSTM-PSO models are biased as a result.

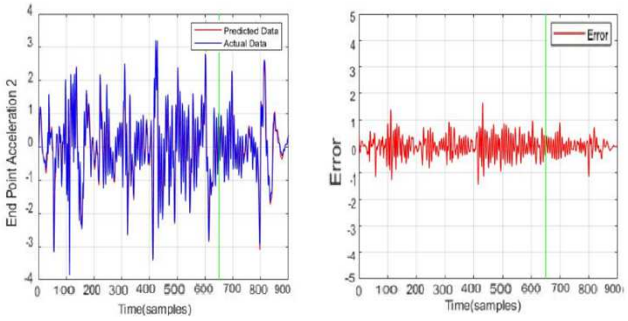

(a) Output and estimated outputs (b) Error between actual and predicted

Fig. 7. Performance of Endpoint accelerations 1 model using LSTM-PSO.

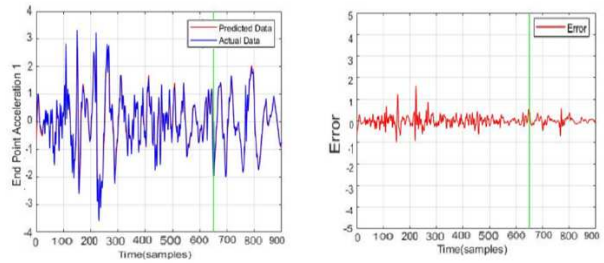

(a) Output and estimated outputs (b) Error between actual and predicted

Fig. 8. Performance of Endpoint accelerations 2 model using LSTM-PSO.

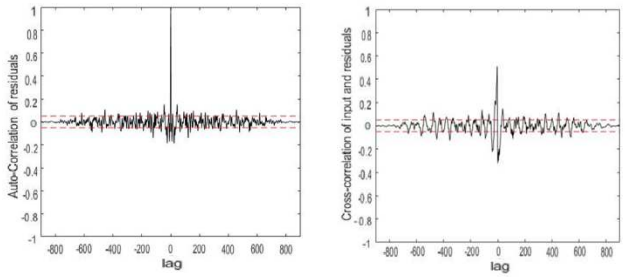

(a) Auto-correlation of residuals (b) Cross-correlation of input and residuals

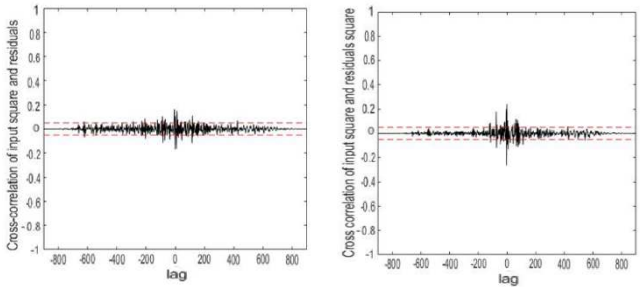

(c) Cross-correlation of input square and residuals (d) Cross correlation of input square and residuals square

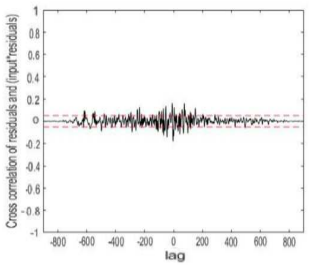

(e) Cross correlation of residuals and (input*residuals)

Fig. 9. Correlation test for endpoint accelerations 1 model using LSTM-PSO.

VI. CONCLUSIONS

The modelling of the endpoint accelerations of TLFM intelligent approaches is presented in this paper. For the purpose of simulating the endpoint accelerations of TLFM, the LSTM-PSO neural network for non-parametric modelling was set into use. The input-output data pairs needed to simulate the TLFM system are collected through the experimental activity. In order to identify the overall TLFM model, the develop TLFM rig was excited using a bang-bang signal. Data from the experimental input and output were obtained and recorded.

Deep learning LSTM improved via particle swarm optimization (PSO) structure depends on a distinct performance indicator, specifically MSE. Implementing LSTM-PSO is simple. The numbers of maximum epoch and neuronal nodes for LSTM-PSO are important factors that must be taken into account during the process.

All of the modelling results are validated using mean square error and correlation testing. Correlation tests and mean square error were used to assess the LSTM-PSO models' capabilities. It has been demonstrated that the LSTM-PSO produces variable mean square error levels in all modelling and validation stages when the numbers of maximum epochs and neural nodes are changed. All of the

modelling results are validated using mean square error and correlation testing. Correlation tests and mean square error were used to assess the LSTM-PSO models' capabilities. It has been demonstrated that the LSTM-PSO produces variable mean square error levels in all modelling and validation stages when the numbers of maximum epochs and neural nodes are changed. It delivered a better model than only LSTM because it was able to predict the system reaction quite accurately. For the endpoint accelerations models of both links 1 and 2, the errors and correlation test are acceptable, with results that are supported by a 95 percent confidence level.

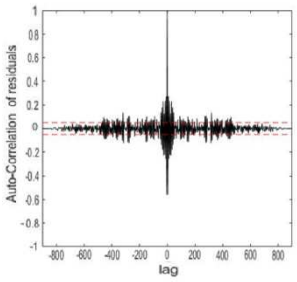

(a) Auto-correlation of residuals

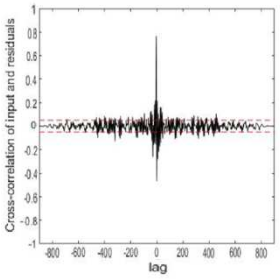

(b) Cross-correlation of input and residuals

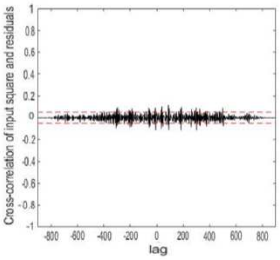

(c) Cross-correlation of input square and residuals

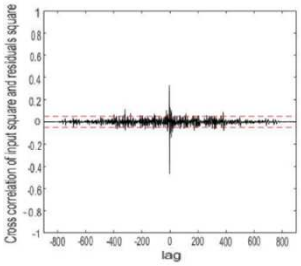

(d) Cross correlation of input square and residuals square

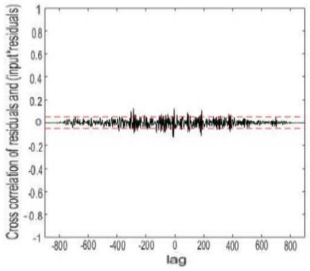

(e) Cross correlation of residuals and (input*residuals)

Fig. 10. Correlation test for endpoint accelerations 2 model using LSTM-PSO.

ACKNOWLEDGMENT

The author would like to acknowledge University Technology Malaysia (UTM) for sponsoring and promoting sustainability necessary to conduct this research.

REFERENCES

[1] Tavakolpour, A. R., Musa Mailah, and IZ Mat Darus. "Active Vibration control of a rectangular flexible plate structure using high gain feedback regulator." *International Review of Mechanical Engineering* 3.5 (2009): 579-587.

[2] Alandoli, E. A., Sulaiman, M., Rashid, M. Z. A., Shah, H. N. M., & Ismail, Z. (2016). A review study on flexible link manipulators. *Journal of Telecommunication, Electronic and Computer Engineering (JTEC)*, *8*(2), 93-97.

[3] Sherstinsky, A., *Fundamentals of recurrent neural network (RNN) and long short-term memory (LSTM) network.* Physica D: Nonlinear Phenomena, 2020. **404**: p. 132306.

[4] Sak, H., A. Senior, and F. Beaufays, *Long short-term memory based recurrent neural network architectures for large vocabulary speech recognition.* arXiv preprint arXiv:1402.1128, 2014.

[5] Liu, N., Li, L., Hao, B., Yang, L., Hu, T., Xue, T., & Wang, S. (2019). Modeling and simulation of robot inverse dynamics using LSTM-based deep learning algorithm for smart cities and factories. *IEEE Access*, *7*, 173989-173998.

[6] Rueckert, E., Nakatenus, M., Tosatto, S., & Peters, J. (2017, November). Learning inverse dynamics models in o (n) time with LSTM networks. In *2017 IEEE-RAS 17th International Conference on Humanoid Robotics (Humanoids)* (pp. 811-816). IEEE.

[7] Xiang, Z., J. Yan, and I. Demir, *A rainfall-runoff model with LSTM-based sequence-to-sequence learning.* Water resources research, 2020. **56**(1): p. e2019WR025326.

[8] Shen, S. L., Atangana Njock, P. G., Zhou, A., & Lyu, H. M. (2021). Dynamic prediction of jet grouted column diameter in soft soil using Bi-LSTM deep learning. *Acta Geotechnica*, *16*(1), 303-315.

[9] Gonzalez, J. and W. Yu, *Non-linear system modeling using LSTM neural networks.* IFAC-PapersOnLine, 2018. **51**(13): p. 485-489.

[10] Wang, Y. *A new concept using LSTM Neural Networks for dynamic system identification*. in *2017 American Control Conference (ACC)*. 2017. IEEE.

[11] Jamali, A., Mat Darus, I. Z., Mohd Samin, P. P., & Tokhi, M. O. (2018). Intelligent modeling of double link flexible robotic manipulator using artificial neural network. *Journal of Vibroengineering*, *20*(2), 1021-1034.

[12] Tan, M., Santos, C. D., Xiang, B., & Zhou, B. (2015). LSTM-based deep learning models for non-factoid answer selection. *arXiv preprint arXiv:1511.04108*.

[13] Ding, G. and L. Qin, *Study on the prediction of stock price based on the associated network model of LSTM.* International Journal of Machine Learning and Cybernetics, 2020. **11**(6): p. 1307-1317.

[14] Darus, I. Z. M., Zahidi Rahman, T. A., & Mailah, M. (2011). Experimental evaluation of active force vibration control of a flexible structure using smart material. *International Review of Mechanical Engineering*, 5(6), p. 1088-1094.

[15] Saad, M. S., Jamaluddin, H., & Mat Darus, I. Z. (2015). Online monitoring and self-tuning control using pole placement method for active vibration control of a flexible beam. *Journal of Vibration and Control*, 21(3), p. 449-460.